

All-Organic Battery Based on Deep Eutectic Solvent and Redox-Active Polymers**

Matthias Uhl⁺,^[a] Sadeeda⁺,^[a] Philipp Penert,^[b] Philipp A. Schuster,^[c] Benjamin W. Schick,^[a] Simon Muench,^[d, e] Attila Farkas,^[a] Ulrich S. Schubert,^[d, e] Birgit Esser,^[b] Alexander J. C. Kuehne,^[c] and Timo Jacob^{*[a, f, g]}

Sustainable battery concepts are of great importance for the energy storage demands of the future. Organic batteries based on redox-active polymers are one class of promising storage systems to meet these demands, in particular when combined with environmentally friendly and safe electrolytes. Deep Eutectic Solvents (DESs) represent a class of electrolytes that can be produced from sustainable sources and exhibit in most cases no or only a small environmental impact. Because of their non-flammability, DESs are safe, while providing an electrochemical stability window almost comparable to established battery electrolytes and much broader than typical aqueous

electrolytes. Here, we report the first all-organic battery cell based on a DES electrolyte, which in this case is composed of sodium bis(trifluoromethanesulfonyl)imide (NaTFSI) and *N*-methylacetamide (NMA) alongside the electrode active materials poly(2,2,6,6-tetramethylpiperidin-1-yl-oxyl methacrylate) (PTMA) and crosslinked poly(vinylbenzylviologen) (X-PVBV²⁺). The resulting cell shows two voltage plateaus at 1.07 V and 1.58 V and achieves Coulombic efficiencies of 98%. Surprisingly, the X-PVBV/X-PVBV⁺ redox couple turned out to be much more stable in NaTFSI:NMA 1:6 than the X-PVBV⁺/X-PVBV²⁺ couple, leading to asymmetric capacity fading during cycling tests.

Introduction

Energy storage systems (ESSs) with their application in portable electronic devices including self-sufficient sensors, electronic consumer goods, and electric vehicles have become well integrated in our daily life. These systems have been significantly improved by the invention of lithium-ion batteries (LiBs).^[1–4] However, these battery systems are commonly composed of lithium, cobalt, and nickel, representing critical raw materials that are rather limited and/or not readily available. Additionally, the production of LiBs requires high thermal energy processes that lead to a large CO₂ footprint.^[4,5] It is imperative to design new energy storage systems that are sustainable and environmentally friendly. For the past two

decades, this challenge has fueled research to find suitable and sustainable alternatives as components of energy storage systems. This includes the development of Deep Eutectic Solvents (DESs) as sustainable electrolytes^[6–8] and redox-active organic electrode materials.^[9–13]

DESs are mixtures of Lewis or Brønsted acids and bases that show a freezing point depression when mixed in their eutectic composition. As a result, these mixtures are liquid at room temperature.^[14] These solvents have properties that could make them suitable as “greener” alternatives to already existing battery electrolytes, as they are non-toxic and biodegradable in most cases.^[15,16] They exhibit low volatility, high thermal stability, low vapor pressure, changeable polarity, and they can be easily prepared.^[17] There are studies that have introduced

[a] M. Uhl,⁺ Sadeeda,⁺ B. W. Schick, Dr. A. Farkas, Prof. Dr. T. Jacob
Institute of Electrochemistry
Ulm University
Albert-Einstein-Allee 47, 89081 Ulm (Germany)
E-mail: timo.jacob@uni-ulm.de

[b] P. Penert, Prof. Dr. B. Esser
Institute of Organic Chemistry II and Advanced Materials
Ulm University
Albert-Einstein-Allee 11, 89081 Ulm (Germany)

[c] P. A. Schuster, Prof. Dr. A. J. C. Kuehne
Institute of Organic and Macromolecular Chemistry
Ulm University
Albert-Einstein-Allee 11, 89081 Ulm (Germany)

[d] Dr. S. Muench, Prof. Dr. U. S. Schubert
Laboratory of Organic and Macromolecular Chemistry
Friedrich Schiller University Jena
Humboldtstrasse 10, 07743 Jena (Germany)

[e] Dr. S. Muench, Prof. Dr. U. S. Schubert
Center for Energy and Environmental Chemistry Jena (CEEC Jena)
Friedrich Schiller University Jena
Philosophenweg 7, 07743 Jena (Germany)


[f] Prof. Dr. T. Jacob
Helmholtz-Institute Ulm (HIU) for Electrochemical Energy Storage
Helmholtzstr. 11, 89081 Ulm (Germany)

[g] Prof. Dr. T. Jacob
Karlsruhe Institute of Technology (KIT)
P.O. Box 3640, 76021 Karlsruhe (Germany)

[*] These authors contributed equally to this work.

[**] A previous version of this manuscript has been deposited on a preprint server (<https://doi.org/10.26434/chemrxiv-2023-nnrc0-v2>)

 Supporting information for this article is available on the WWW under <https://doi.org/10.1002/cssc.202301057>

 © 2023 The Authors. ChemSusChem published by Wiley-VCH GmbH. This is an open access article under the terms of the Creative Commons Attribution Non-Commercial NoDerivs License, which permits use and distribution in any medium, provided the original work is properly cited, the use is non-commercial and no modifications or adaptations are made.

DESs in LiBs^[18] as well as in sodium-ion batteries.^[19] Previously, the DES composed of sodium *bis*(trifluoromethanesulfonyl) imide (NaTFSI) and *N*-methylacetamide (NMA) in the eutectic molar ratio 1:6, which is also used in this study, has proved to be a viable electrolyte in half-cell investigations with poly-(2,2,6,6-tetramethylpiperidin-1-yl-oxylmethacrylate) (PTMA) electrodes.^[20] However, these solvents had, to the best of our knowledge, so far not yet been paired with polymer electrodes for the construction of an all-organic energy storage system.

Research on organic-based batteries began roughly 45 years ago,^[21,22] but was discontinued soon.^[23] The discovery of high-capacity polymers such as PTMA,^[24] paired with relatively high discharge voltages, again fueled the interest in organic electrode materials resulting in various energy storage applications.^[25–31] Today, PTMA is one of the most prominent radical-based redox-active polymers. It is used as positive electrode, containing a stabilized nitroxyl radical known as 2,2,6,6-tetramethylpiperidiny-*N*-oxyl (TEMPO). This radical has excellent electrochemical properties and the required stability.^[32] PTMA was first used in a lithium organic battery with an average discharge voltage of 3.5 V and a discharge capacity of 77 mAh g⁻¹.^[24] The negative electrode of the all-organic full battery cell in this study was a viologen-based polymer containing a double-positively charged cation in its pristine state, which is reduced to the neutral species after undergoing two single-electron transfer steps.^[5] We used the crosslinked polymer poly(*N*-(4-vinylbenzyl)-*N'*-methylviologen) (X-PVBV²⁺) in this case to hinder dissolution in the solvent.^[33] This combination of PTMA as positive and X-PVBV²⁺ as negative electrode leads to an all-organic battery operating in an anion rocking-chair configuration, which is a rare cell-type that can be realized with organic electrode materials.^[34] In contrast to cation rocking-chair or dual-ion batteries, only the anion is used as charge carrier. Other reports of such anion rocking-chair all-organic cells also use viologen-based compounds as negative electrodes, both with aqueous^[35–38] and non-aqueous electrolytes,^[39–41] since viologen is a rare example for a *p*-type organic electrode material with a low redox potential. In general, anion rocking-chair batteries exhibit high theoretical energy densities at comparably low cost because of their high abundance compared to many metals. Due to the more covalent character of the anion bonding in the electrode material, they exhibit higher flexibility for different storage concept like intercalation and conversion. On the other hand, especially with large anions, repeating insertion into the electrode material leads to significant changes in volume and with this to dismantling of the electrode shortening the cycling life of the battery.^[42] One combination of a TEMPO- and a viologen-based polymer was realized in organic redox flow batteries with an aqueous electrolyte resulting in a cell with a discharge voltage of 1.3 V and a discharge capacity of 44 mAh, showing a stable performance over 100 cycles, but using only half of the capacity of the viologen polymer.^[43] For increasing the energy density, electrolytes with a larger stability window than water are needed to make the use of the second redox-process of the viologen polymer possible. In general, new, tailor-made electrolytes with high ionic conductivity at room temperature and larger electro-

chemical stability windows are needed to enhance anion rocking-chair batteries.^[42] One possible option would therefore be the use of DESs.

In the present study, we combine a DES with redox-active polymers to build the first all-organic battery of this kind. As depicted in Figure 1, two redox-active polymers have been combined with a deep eutectic solvent synthesized from NaTFSI and NMA in the molar ratio 1:6. Combining the DES with PTMA and X-PVBV²⁺ enables using both redox events of X-PVBV²⁺ within the electrochemical stability window of the DES electrolyte. With this, we could prove the applicability of DESs for all-organic batteries based on cyclic voltammetry of battery half-cells and galvanostatic cycling of full cells showing a high Coulombic efficiency of 98%. The oxidation of the monovalent ion X-PVBV⁺ to the fully-oxidized state seems to be unfavorable compared to the first oxidation of X-PVBV during cycling in the DES, resulting in asymmetrical capacity fading for the two redox processes of X-PVBV²⁺.

Results and Discussion

The two polymers PTMA and X-PVBV²⁺ (molecular structures and redox reactions given in Figure S1) were first investigated in half-cells using cyclic voltammetry before assembling full cells. As electrolyte, the DES NaTFSI:NMA in its eutectic ratio 1:6 was selected. The choice of this DES is based on its thermal, physical, and electrochemical characterization.^[19,20] Indeed, the eutectic ratio 1:6, which was determined by differential scanning calorimetry, turned out to be the best choice in terms of electrochemical stability and ionic conductivity in contact with PTMA-based electrodes.^[20] The respective voltammograms for the combination of the DES with the here used polymers in half-cells indicate high electrochemical activity. Representatives of these studies are depicted in Figure 2 showing the electrochemical behavior of both polymers as active materials in composite electrodes in separate half-cells on the same potential scale. Further voltammograms at different scan rates are shown in Figure S2. Details on the electrode composition and fabrication can be found in the experimental section. More fundamental information on the used polymers and electrodes can be found elsewhere.^[20,44,45]

X-PVBV²⁺ exhibits two separate redox events at -0.44 V and -0.95 V vs. a Ag pseudo-reference electrode as respective redox potentials. These two steps represent the two successive single electron transfer processes starting from the divalent cation to the neutral polymer and the other way around.^[46] PTMA can be oxidized from its neutral radical form to the monovalent cation. This process occurs with high activity, small peak separation, and quasi-reversibility as shown in different electrolytes including the DES of interest.^[20,44,46] The redox potential of PTMA is found at 0.63 V vs. Ag, and with this 1.07 V, respectively 1.58 V, more positive than the two redox processes of X-PVBV²⁺. Therefore, PTMA acts as positive and X-PVBV²⁺ as negative electrode in the resulting full cells.

When assembling the respective full cell in a two-electrode setup together with the eutectic mixture of NaTFSI:NMA as

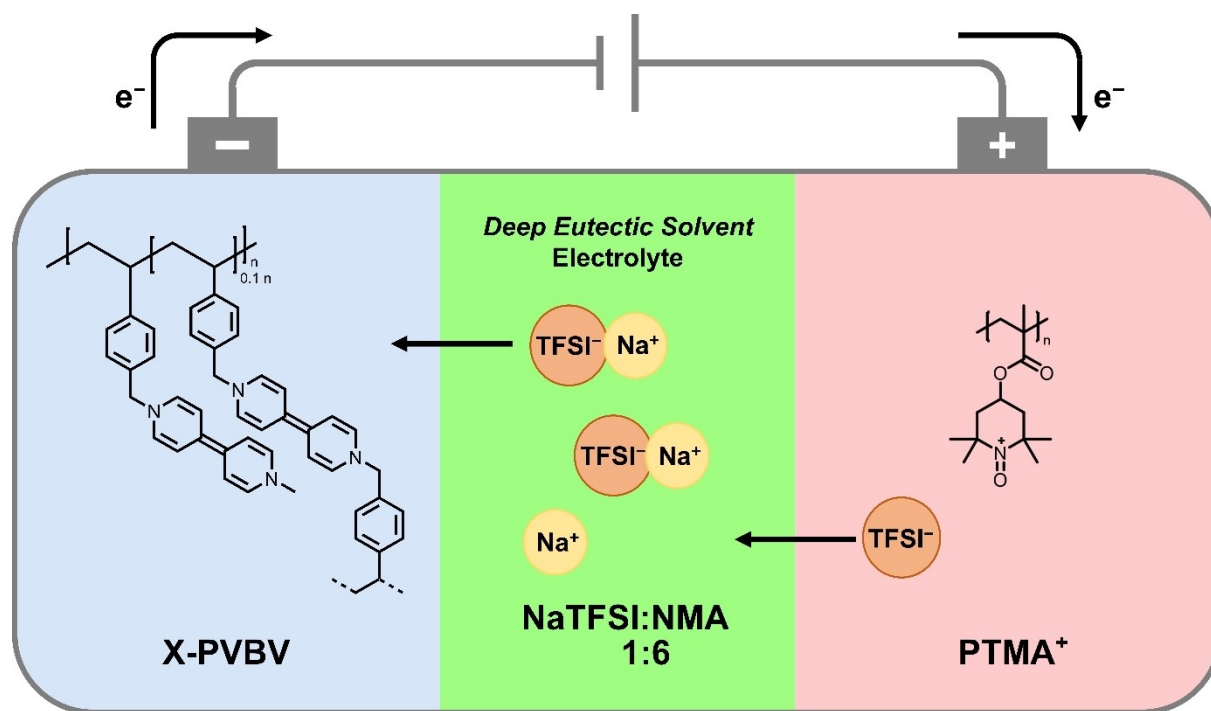


Figure 1. Schematic figure of the charged all-organic battery composed of the DES NaTFSI:NMA 1:6 as electrolyte, PTMA as active material in the positive electrode and X-PVBV²⁺ as active material in the negative electrode. Electron and ion movement indicates the discharge process.

electrolyte taking X-PVBV²⁺ as the capacity-limiting electrode, both redox steps of X-PVBV²⁺ can be well observed in the voltage profile, as depicted in Figure 3. The resulting voltage plateaus during charge and discharge fit well to the expectation from cyclic voltammetry of the half-cells. The charging and discharging voltages deviate only little from the previously determined potential differences due to the overpotentials of the electron transfer and charge transport. The influence of the

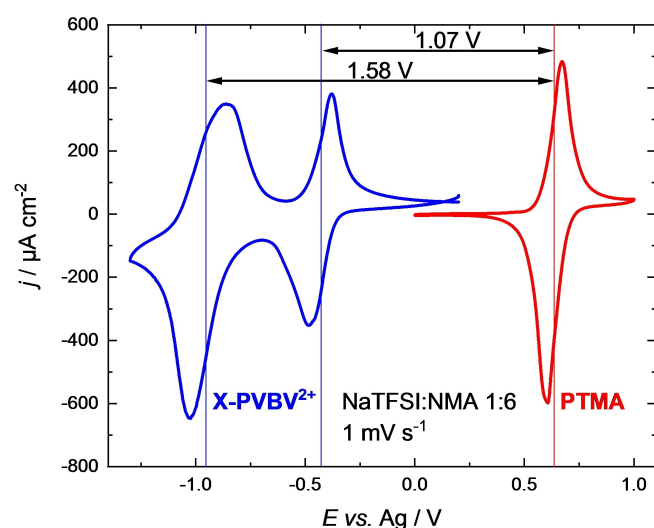


Figure 2. Cyclic voltammograms of X-PVBV²⁺- (blue) and PTMA- (red) based composite electrodes in half-cells vs. Ag pseudo-reference electrode with the DES NaTFSI:NMA in its eutectic molar ratio 1:6 as electrolyte at a scan rate of 1 mV s⁻¹.

diffusion of the ions in the electrolyte on the electrochemical behavior is also reflected in the Warburg-like shape of the electrochemical impedance spectrum at low frequencies (Figure S3). Therefore, at a C-rate of 10, discharging occurs roughly at 1.5 V and 1.0 V, respectively.

The voltage profile reflects the high Coulombic efficiency of this all-organic full cell since charge and discharge capacity are almost identical. Recording 100 cycles at a C-rate of 10 (Figure 4), the Coulombic efficiency remains stable at ~98%, which is even higher than for a comparable organic battery system based on a TEMPO-polymer and a polyviologen using an aqueous electrolyte and excluding the plateau at higher voltage resulting in 95% Coulombic efficiency.^[35] Compared to other non-aqueous electrolytes, the efficiency of our full cell is not as good as that of other TEMPO- or viologen-based polymers in half-cells,^[40,44,47] but can definitely compete with and in most cases even surpass other all-organic battery full cells of the anion rocking-chair type.^[39–41,47]

By contrast, the discharge capacity is not that stable. Within the first ten to twenty cycles, the capacity increases, which is most probably connected to a proceeding wetting of the electrodes.^[20] Additionally, the exchange of the PF₆⁻ ions being present in the freshly synthesized X-PVBV²⁺ polymer by the TFSI⁻ ions from the electrolyte could contribute to this increase in capacity. Afterwards, the capacity is steadily decreasing to ~50% of its initial value after 100 cycles. The reason for this might be mainly an instability of the X-PVBV²⁺ cation in the DES, as also reported by Cadiou *et al.*,^[41] who investigated crosslinked viologen-based polymers in 1 M LiClO₄ in propylene carbonate. They attribute this behavior to steric and electronic

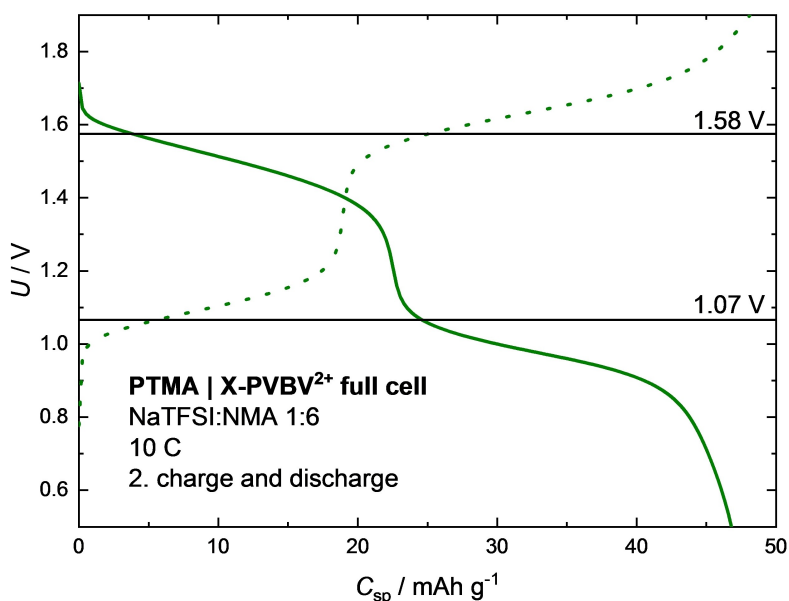


Figure 3. Voltage profile for the second galvanostatic charge (dashed line) and discharge (solid line) of the X-PVBV²⁺ | PTMA full cell with the DES NaTFSI:NMA in its eutectic molar ratio 1:6 as electrolyte at a rate of 10 C. The black lines indicate the potential differences between the redox events of PTMA and X-PVBV²⁺ extracted from cyclic voltammetry (Figure 2).

hindrance for the uptake of the second anion during oxidation to the bivalent cation. Fittingly, according to Figure S4, the lower voltage plateau representing the X-PVBV⁺/X-PVBV²⁺ couple diminishes much faster compared to the high voltage one. This might also explain the initial increase in capacity during the first cycles. If the DES interacts more strongly with the monovalent cation and if the uptake of a second anion per viologen unit is unfavorable, the wetting process is enhanced after the first reduction. Therefore, even after 16 h at OCP in the fully-oxidized state of X-PVBV²⁺, there is still room for activation

of the electrode, which is reflected by the increasing capacity of the high voltage plateau within the first cycles (Figure S4).

Apart from this, also the capacity of the high-voltage plateau slightly decreases after reaching the maximum capacity. After 100 cycles, the capacity of the high-voltage plateau decreased roughly to 80% of its initial value indicating much higher stability of the first oxidation state compared to the fully-oxidized X-PVBV²⁺ in the DES. The capacity loss for the high voltage plateau might either be caused by polymer dissolution in the electrolyte or by partial passivation of the

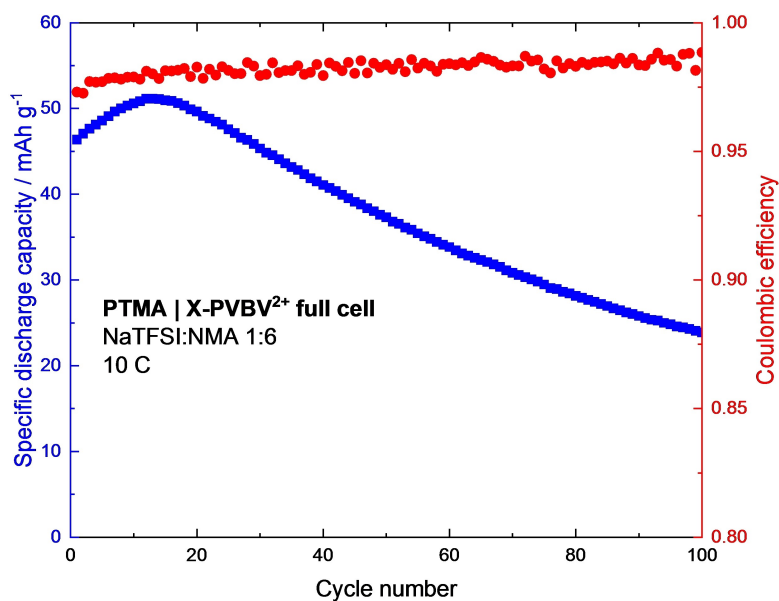


Figure 4. Galvanostatic charge-discharge cycling of the X-PVBV²⁺ | PTMA full cell with the DES NaTFSI:NMA in its eutectic molar ratio 1:6 as electrolyte at a rate of 10 C showing the specific discharge capacity (blue) and the Coulombic efficiency (red) for 100 cycles.

electrode, as was already discussed previously.^[20] An additional reason could be the mechanical stress in the X-PVBV²⁺ polymer during the unfavorable uptake of the second TFSI⁻ anion by complete discharge leading to irreversible processes, which is generally assumed to be a problem for anion rocking-chair batteries.^[42] The potential profiles of the anode half-cell shown in Figure S5 give evidence, that this behavior of the full cell is almost exclusively influenced by the X-PVBV²⁺ polymer. As for the full cell, the capacity of the X-PVBV/X-PVBV⁺ potential step at roughly -0.9 V decreases slower than for X-PVBV⁺/X-PVBV²⁺ at -0.4 V. Since only the discharge is depicted, the mentioned potentials do not exactly fit the redox potentials extracted from cyclic voltammetry, but the peak currents of the oxidation of X-PVBV in Figure 2. Interestingly, the higher stability of the X-PVBV/X-PVBV⁺ couple compared to the X-PVBV⁺/X-PVBV²⁺ one is as mentioned in agreement with findings in carbonate-based electrolytes,^[41] but in contrast to the findings in aqueous electrolytes, where the reduction to the neutral viologen species was excluded due to stability reasons.^[46] For eutectic solvents, unexpected stabilization of ions was also observed for Cu⁺ ions in a chlorine-free DES, which as well contradicts the common behavior in aqueous media.^[48]

When switching to a rate of 1 C after 15 cycles at 10 C (Figure S6), the discharge capacity immediately reaches its maximum in the first slow cycle. But the price of the high capacity is a lower Coulombic efficiency of 90% at its best and faster degradation. The slower the cycling, the more pronounced is the capacity decrease. Again, the dismantling of the electrode by complete discharging leading to mechanical stress by the anion insertion can cause this effect. Low rates allow anion diffusion and insertion into deeper layers of the electrode, causing more lasting damage to the electrode structure than with faster cycling. This is also the reason why it was possible to cycle a battery based on a TEMPO- combined with a viologen-polymer 2000 times with a much faster rate of 60 °C and using smaller anions in aqueous media.^[35]

Conclusions

Using poly(2,2,6,6-tetramethylpiperidin-1-yl-oxyl methacrylate) (PTMA) as positive electrode and crosslinked poly(vinylbenzylviologen) (X-PVBV²⁺) as negative electrode, we have proven the applicability of Deep Eutectic Solvents (DESs) as electrolytes for sustainable all-organic batteries using sodium bis(trifluoromethanesulfonyl) imide (NaTFSI) and *N*-methylacetamide (NMA) in its eutectic molar ratio of 1:6. The full cells, operating in anion rocking-chair mode, well match the expectations from cyclic voltammetry measurements by showing voltage plateaus at roughly 1.07 V and 1.58 V, perfectly matching the redox-potential differences of the polymers in half-cells. The Coulombic efficiency of the resulting all-organic battery reaches 98% at a C-rate of 10 for at least 100 cycles. The fading capacity can be mainly attributed to the hindrance of the second ion insertion in X-PVBV⁺ during cycling in the DES under investigation, causing a decrease of the capacity of the low voltage plateau. The redox event at 1.58 V exhibits a much

higher stability with roughly 80% of the initial capacity after 100 cycles.

These results open new opportunities for the use of DESs in all-organic batteries. Regarding the choice of DES, the redox-potential but as well the stability and solubility of the used polymers in their different oxidation states are decisive for the battery performance. The wide variation possibilities of DESs and redox-active polymers illustrates the potential of this type of battery. The challenge remains to identify suitable combinations based on a fundamental understanding of the interactions between the different battery components.

Experimental Section

Preparation of the Electrolyte: The electrolyte was prepared and kept in a glovebox (M. Braun, H₂O < 0.5 ppm, O₂ < 0.5 ppm) filled with nitrogen gas. *N*-Methylacetamide (Aldrich chemicals, 99%, further purified by distillation) was melted at 50 °C. 1.5 g of sodium bis(trifluoromethanesulfonyl) imide (Solvionic, 99.9%) was added to 2.17 g of NMA and stirred until the mixture was homogenous. For drying, the mixture was kept over 4 Å molecular sieve (Merck) for over two weeks. The resulting water content was determined using Karl-Fischer-Titration (KF-Coulmeter 851 by Metrohm, with Hydranal Coulmat AG electrolyte by Honeywell) to lie below 10 ppm.

Preparation of the Electrodes: The preparation of the positive electrodes was performed analogue to our previously reported procedure.^[20] The mass loading was between 0.33 mg cm⁻² and 0.45 mg cm⁻² of PTMA. The slurries for the negative electrode were fabricated by mixing X-PVBV²⁺ with the conductive additive Timcal Super C65 and the binder polyvinylidene fluoride (PVdF) (Solef 5130, BASF) in the mass ratio 60:30:10 in *N*-methyl-2-pyrrolidone (NMP) (99.5%, extra dry over molecular sieve, AcroSeal, Thermo scientific). A brief description of the synthesis of X-PVBV²⁺ is provided in the supporting information. Further information will be published elsewhere.^[45] The resulting slurries were coated on Al-foil which was etched with 5 wt% KOH solution prior to use. For drying, the electrodes were kept at 80 °C under vacuum overnight. The mass loading for X-PVBV²⁺ was between 0.33 mg cm⁻² and 0.4 mg cm⁻².

Cell-Assembly and Electrochemical Measurements: The electrochemical measurements were conducted in a nitrogen-filled glovebox using Swagelok-type cells in a three-electrode setup for cyclic voltammetry and a two-electrode setup for galvanostatic full cell tests with a geometrical electrode area of 1.13 cm² except for the reference electrode. Glass fiber separators (Whatman, GF/B) were placed between the electrodes and soaked with 60 μL of electrolyte each. For the half-cells, graphite disks (Goodfellow, 99.997%) were used as counter electrodes and freshly annealed Ag-wires (MaTeck, 99.99%) as reference electrodes. After the assembly, the half-cells were left for equilibration for two to 16 hours, full cells for 16 hours so the potential of the electrodes could stabilize. Then, the cell was connected to an Interface 1010B potentiostat (Gamry Instruments). Details for the individual measurements are given in the caption of the respective figures. For the galvanostatic measurements, C-rates were calculated based on the theoretical capacity of the capacity limiting electrode. The specific capacities of the full cells are given with respect to the mass of X-PVBV²⁺, which is the active material of the capacity limiting electrode.

Supporting Information

Supporting Information is available from the Wiley Online Library or from the author.

Acknowledgements

This work contributes to the research performed at CELEST (Center for Electrochemical Energy Storage Ulm-Karlsruhe) and was funded by the German Research Foundation (DFG) under Project ID 390874152 (POLiS Cluster of Excellence) as well as the priority program SPP 2248 Polymer-based Batteries (Project IDs 441209207 and 441236036). Open Access funding enabled and organized by Projekt DEAL.

Conflict of Interests

The authors declare no conflict of interest.

Data Availability Statement

The data that support the findings of this study are available from the corresponding author upon reasonable request.

Keywords: all-organic battery · electrochemistry · sustainable chemistry · polymers · deep eutectic solvents

- [1] M. S. Whittingham, *Chem. Rev.* **2004**, *104*, 4271–4302.
- [2] J. B. Goodenough, *Nat. Electron.* **2018**, *1*, 204.
- [3] A. Yoshino, *Angew. Chem. Int. Ed.* **2012**, *51*, 5798–5800.
- [4] C. Friebe, A. Lex-Balducci, U. S. Schubert, *ChemSusChem* **2019**, *12*, 4093–4115.
- [5] M. D. Hager, B. Esser, X. Feng, W. Schuhmann, P. Theato, U. S. Schubert, *Adv. Mater.* **2020**, *32*, 2000587.
- [6] J. Wu, Q. Liang, X. Yu, Q. Lü, L. Ma, X. Qin, G. Chen, B. Li, *Adv. Funct. Mater.* **2021**, *31*, 2011102.
- [7] S. Azmi, M. F. Koudahi, E. Frackowiak, *Energy Environ. Sci.* **2022**, *15*, 1156–1171.
- [8] M. H. Chakrabarti, F. S. Mjalli, I. M. Alnashef, M. A. Hashim, M. A. Hussain, L. Bahadori, C. T. J. Low, *Renewable Sustainable Energy Rev.* **2014**, *30*, 254–270.
- [9] D. Larcher, J.-M. Tarascon, *Nat. Chem.* **2015**, *7*, 19–29.
- [10] F. Otteny, V. Perner, D. Wassy, M. Kolek, P. Bieker, M. Winter, B. Esser, *ACS Sustainable Chem. Eng.* **2020**, *8*, 238–247.
- [11] J. Kim, J. H. Kim, K. Ariga, *Joule* **2017**, *1*, 739–768.
- [12] M. E. Bhosale, S. Chae, J. M. Kim, J. Y. Choi, *J. Mater. Chem. A* **2018**, *6*, 19885–19911.
- [13] B. Esser, *Org. Mater.* **2019**, *01*, 063–070.
- [14] E. L. Smith, A. P. Abbott, K. S. Ryder, *Chem. Rev.* **2014**, *114*, 11060–11082.
- [15] K. Radošević, M. Cvjetko Bubalo, V. Gaurina Srček, D. Grgas, T. Landeka Dragičević, R. I. Redovniković, *Ecotoxicol. Environ. Saf.* **2015**, *112*, 46–53.
- [16] S. Khandelwal, Y. K. Tailor, M. Kumar, *J. Mol. Liq.* **2016**, *215*, 345–386.
- [17] B. B. Hansen, S. Spittle, B. Chen, D. Poe, Y. Zhang, J. M. Klein, A. Horton, L. Adhikari, T. Zelovich, B. W. Doherty, B. Gurkan, E. J. Maginn, A. Ragauskas, M. Dadmun, T. A. Zawodzinski, G. A. Baker, M. E. Tuckerman, R. F. Savinell, J. R. Sangoro, *Chem. Rev.* **2021**, *121*, 1232–1285.
- [18] A. Boisset, S. Menne, J. Jacquemin, A. Balducci, M. Anouti, *Phys. Chem. Chem. Phys.* **2013**, *15*, 20054–20063.
- [19] D. De Sloovere, D. E. P. Vanpoucke, A. Paulus, B. Joos, L. Calvi, T. Vranken, G. Reekmans, P. Adriaensens, N. Eshraghi, A. Mahmoud, F. Boschini, M. Safari, M. K. Van Bael, A. Hardy, *Adv. Energy Sustain. Res.* **2022**, *3*, 2100159.
- [20] M. Uhl, T. Geng, P. A. Schuster, B. W. Schick, M. Kruck, A. Fuoss, A. J. C. Kuehne, T. Jacob, *Angew. Chem. Int. Ed.* **2023**, *62*, e202214927.
- [21] H. Shirakawa, E. J. Louis, A. G. MacDiarmid, C. K. Chiang, A. J. Heeger, *J. Chem. Soc. Chem. Commun.* **1977**, 578–580.
- [22] C. K. Chiang, Y. W. Park, A. J. Heeger, H. Shirakawa, E. J. Louis, A. G. MacDiarmid, *J. Chem. Phys.* **1978**, *69*, 5098–5104.
- [23] J. S. Miller, *Adv. Mater.* **1993**, *5*, 671–676.
- [24] K. Nakahara, S. Iwasa, M. Satoh, Y. Morioka, J. Iriyama, M. Suguro, E. Hasegawa, *Chem. Phys. Lett.* **2002**, *359*, 351–354.
- [25] Y. Xu, Y. Wen, J. Cheng, G. Cao, Y. Yang, *Electrochem. Commun.* **2009**, *11*, 1422–1424.
- [26] Z. Li, S. Li, S. Liu, K. Huang, D. Fang, F. Wang, S. Peng, *Electrochem. Solid-State Lett.* **2011**, *14*, A171–A173.
- [27] D. Mecerreyes, L. Porcarelli, N. Casado, *Macromol. Chem. Phys.* **2020**, *221*, 1900490.
- [28] A. Molina, N. Patil, E. Ventosa, M. Liras, J. Palma, R. Marcilla, *Adv. Funct. Mater.* **2020**, *30*, 1–11.
- [29] O. Buyukcakir, J. Ryu, S. H. Joo, J. Kang, R. Yuksel, J. Lee, Y. Jiang, S. Choi, S. H. Lee, S. K. Kwak, S. Park, R. S. Ruoff, *Adv. Funct. Mater.* **2020**, *30*, 1–11.
- [30] X. Zhang, Z. Xiao, X. Liu, P. Mei, Y. Yang, *Renewable Sustainable Energy Rev.* **2021**, *147*, 111247.
- [31] P. Jezowski, O. Crosnier, E. Deunf, P. Poizot, F. Béguin, T. Brousse, *Nat. Mater.* **2018**, *17*, 167–173.
- [32] S. Muench, A. Wild, C. Friebe, B. Häupler, T. Janoschka, U. S. Schubert, *Chem. Rev.* **2016**, *116*, 9438–9484.
- [33] D. Nataraj, R. Reddy, N. Reddy, *Eur. Polym. J.* **2020**, *124*, 109484.
- [34] P. Poizot, F. Dolhem, J. Gaubicher, *Curr. Opin. Electrochem.* **2018**, *9*, 70–80.
- [35] K. Koshika, N. Chikushi, N. Sano, K. Oyaizu, H. Nishide, *Green Chem.* **2010**, *12*, 1573–1575.
- [36] N. Chikushi, H. Yamada, K. Oyaizu, H. Nishide, *Sci. China Chem.* **2012**, *55*, 822–829.
- [37] N. Sano, W. Tomita, S. Hara, C. M. Min, J. S. Lee, K. Oyaizu, H. Nishide, *ACS Appl. Mater. Interfaces* **2013**, *5*, 1355–1361.
- [38] S. Peticarari, E. Grange, T. Doizy, Y. Pellegrin, E. Quarez, K. Oyaizu, A. J. Fernandez-Ropero, D. Guyomard, P. Poizot, F. Odobel, J. Gaubicher, *Chem. Mater.* **2019**, *31*, 1869–1880.
- [39] M. Yao, H. Sano, H. Ando, T. Kiyobayashi, *Sci. Rep.* **2015**, *5*, 1–8.
- [40] A. Jouhara, E. Quarez, F. Dolhem, M. Armand, N. Dupré, P. Poizot, *Angew. Chem. Int. Ed.* **2019**, *58*, 15680–15684.
- [41] V. Cadiou, A. C. Gaillot, É. Deunf, F. Dolhem, L. Dubois, T. Gutel, P. Poizot, *ChemSusChem* **2020**, *13*, 2345–2353.
- [42] Q. Liu, Y. Wang, X. Yang, D. Zhou, X. Wang, P. Jaumaux, F. Kang, B. Li, X. Ji, G. Wang, *Chem.* **2021**, *7*, 1993–2021.
- [43] T. Hagemann, J. Winsberg, M. Grube, I. Nischang, T. Janoschka, N. Martin, M. D. Hager, U. S. Schubert, *J. Power Sources* **2018**, *378*, 546–554.
- [44] S. Muench, P. Gerlach, R. Burges, M. Strumpf, S. Hoepfner, A. Wild, A. Lex-Balducci, A. Balducci, J. C. Brendel, U. S. Schubert, *ChemSusChem* **2021**, *14*, 449–455.
- [45] M. E. Bhosale, C. Schmidt, P. Penert, G. Studer, B. Esser, *ChemRxiv* **2023**, 10.26434/chemrxiv-2023-5nx25..
- [46] T. Janoschka, S. Morgenstern, H. Hiller, C. Friebe, K. Wolkersdörfer, B. Häupler, M. D. Hager, U. S. Schubert, *Polym. Chem.* **2015**, *6*, 7801–7811.
- [47] T. P. Nguyen, A. D. Easley, N. Kang, S. Khan, S.-M. Lim, Y. H. Rezenom, S. Wang, D. K. Tran, J. Fan, R. A. Letteri, X. He, L. Su, C.-H. Yu, J. L. Lutkenhaus, K. L. Wooley, *Nature* **2021**, *593*, 61–66.
- [48] T. Geng, B. W. Schick, M. Uhl, A. J. C. Kuehne, L. A. Kibler, M. U. Cebelin, T. Jacob, *ChemElectroChem* **2022**, *9*, e202101263.

Manuscript received: July 27, 2023

Accepted manuscript online: July 28, 2023

Version of record online: October 26, 2023